Analysis and Design of enhanced DFT-Based Controller for Selective Harmonic Compensation in Active Power Filters

Hao Chen, Huawu Liu, Yan Xing, Haibing Hu
Center for More-Electric-Aircraft Power System
Nanjing University of Aeronautics and Astronautics
Nanjing, China
Email: chenhao@nuaa.edu.cn

Kai Sun
State Key Lab of Power Systems, Department of Electrical Engineering
Tsinghua University
Beijing, China
Email: sun-kai@mail.tsinghua.edu.cn

***Abstract*—Traditional Discrete Fourier Transform(DFT)-based repetitive controller is widely used in active power filters(APF) thanks to its unique merits such as excellent selectivity and simplicity. However, the structure of the only one feedback path results in the same steps of leading angles for all harmonic frequencies. Since the phase response may not be proportional to frequency and the gain of the plant varies with frequency, identical leading angles and gain coefficients can't compensate the phase lag and the gain attenuation effectively at different harmonics. All those facts imply constraints to obtain the best stability margins and performance. The proposed controller provides feedback path and gain coefficient for each harmonic according to the characteristics of the plant respectively. In addition, the correction term is embedded in the forward channel to provide overall phase compensation and correct the plant for better characteristics. As a result, the novel control structure incorporated in sliding DFT can improve the performance greatly. Detailed design consideration is given with focus on stability analysis and transient behavior of the APF. Experimental results validate the effectiveness of the theoretical analysis.**

Keywords—active power filter; closed-loop; selective harmonic compensation; DFT-Based controller

I. INTRODUCTION

In contrast to the load-current detection type, APF with source-current detection is usually considered as closed-loop systems, as shown in Fig.2. The closed-loop system of APF provides many advantages such as better harmonic compensating performance and lower demands for fast current control loop [1]. In order to reduce the rating of APF and minimize the APF interactions with possible dynamic components of the load [2], selective harmonic compensation is preferred in practice. Many research works have been carried out to implement closed-loop selective harmonic control strategies [1]-[7]. Traditional DFT-based repetitive controller has been widely applied to APF [3], featuring excellent selectivity and simplicity [8].

However, defective structure of traditional controller makes it difficult to achieve the best stability margins and performance. Besides, control parameters need to be optimized according to the frequency characteristics of the plant. Those drawbacks are overcome by the proposed enhanced DFT-based controller with optimized design consideration given in this paper.

This work was funded by National Natural Science Foundation of China(51577088).

II. PROPOSED ENHANCED DFT-BASED CONTROLLER

The closed-loop control block diagram of APF is illustrated in Fig.2, where $G_{DFT}(z)$ is the DFT-based controller, $G_{ic}(z)$ is the proportional integral controller(PI) of current loop, $G_p(z)$ is the plant model, $r(z)$ is the current reference command, $e(z)$ is the error signal, $i_C(z)$ is the compensation current, $i_L(z)$ is the load current, $i_S(z)$ is the grid current, $v_{dc}(z)$ is the voltage of dc side, $H_{PI}(z)$ is the PI controller of voltage loop, $i_{dc}^*(z)$ is the active component used for controlling the voltage of dc side and the current reference direction is shown in Fig.1.

Fig.3 shows the block diagram of traditional DFT-based controller, where $F_{DFT}(z)$ can be expressed as follows,

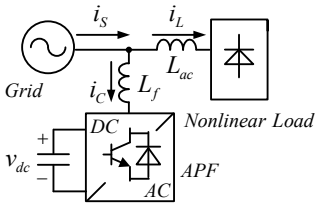

Fig. 1: Shunt APF topology

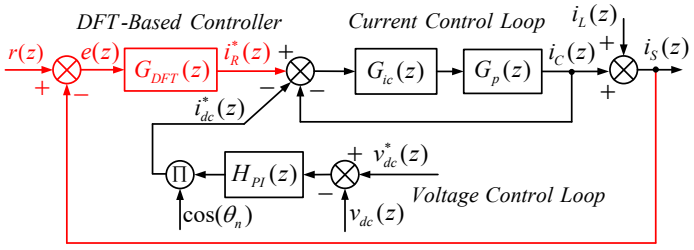

Fig. 2: APF closed-loop control system

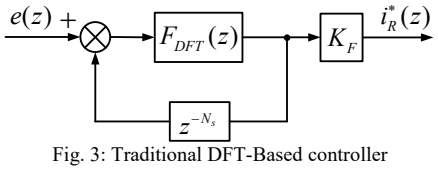

Fig. 3: Traditional DFT-Based controller

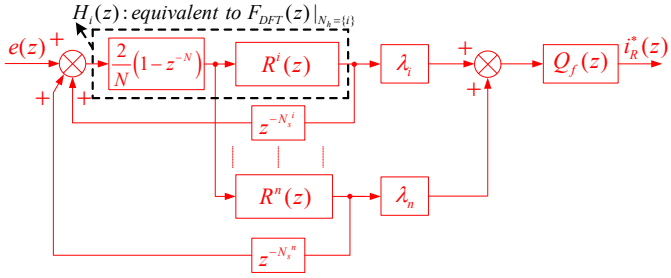

Fig.4: Proposed enhanced DFT-Based Controller

$$F_{DFT}(z)=\frac{2}{N}\sum_{k=0}^{N-1}\left\{\sum_{i\in N_h}\cos[\frac{2\pi}{N}i(k+N_s)]\right\}\cdot z^{-k} \tag{1}$$

in which N_h is the set of selected harmonic frequencies, N is the number of samples per fundamental period, i is the harmonic order, N_s is the number of leading steps.

Fig.4 shows the specific composition of the proposed DFT controller, where N_s^i is the step of leading phase compensating for phase lag at i^{th} harmonic, N_h is the set of harmonic orders need to be restrained, λ_i is the correction factor used for tuning the gain of DFT controller at i^{th} harmonic, and $Q_f(z)$ is the corrective function. The key part of DFT controller $R^i(z)$ can be written as,

$$R^i(z)=\frac{\cos(\frac{2\pi}{N}i\cdot N_s^{\,i})-\cos[\frac{2\pi}{N}i\cdot(1-N_s^{\,i})]\cdot z^{-1}}{1-2\cos(\frac{2\pi}{N}i)\cdot z^{-1}+z^{-2}},\quad i\in N_h \tag{2}$$

The proposed controller is based on sliding DFT to reduce the calculation burden [7]-[14], which provides various outstanding advantages as follows over the traditional DFT-based controller.

- The feedback path and gain coefficient λ_i are introduced for each harmonic according to the characteristics of the plant at different frequencies respectively in the proposed controller, while those parameters must be identical for all frequencies in the traditional controller, as shown in Fig.3.
- The proposed controller provides $Q_f(z)$ in forward channel to correct the plant for better characteristics.

As a matter of fact, the traditional controller is equivalent to the proposed controller if N_s^i and λ_i are identical and $Q_f(z)$ are equal to one. Optimized design consideration will be given in the next section to make full use of the advantages of the proposed controller.

III. Analysis and Design of Proposed Controller

A. Stability analysis

As Fig.2 shows, the error transfer function $G_e(z)$ for the system can be derived as follows,

$$\begin{aligned}G_e(z)&=\frac{e(z)}{r(z)-i_L(z)}\\&=\frac{1-\sum_{i\in N_h}H_i(z)\cdot z^{-N_s^i}}{1-\sum_{i\in N_h}\{H_i(z)\cdot z^{-N_s^i}[1-\lambda_i\cdot z^{N_s^i}\cdot G_{ip}(z)\cdot Q_f(z)]\}}\forall i\in N_h\end{aligned} \tag{3}$$

where $H_i(z)=\frac{2}{N}\cdot(1-z^{-N})\cdot R^i(z)$, $H_i(z)$ represents the DFT with N_s^i steps of leading phase provided, N_h is the set of harmonic orders need to be restrained, and $G_{ip}(z)=\frac{G_{ic}(z)G_p(z)}{1+G_{ic}(z)G_p(z)}(1+\Delta z)$, Δz represents the modeling error. Suppose that there exists a constant ε such that $\|\Delta z\|<\varepsilon$. Let $\Delta z=\|z\|e^{j\theta_\Delta(\omega)}$ to estimate the model error.

Obviously, the stability condition of current loop should be firstly met. According to (3) and small gain theorem [15], additional condition should be satisfied as follows to ensure the stability of system.

$$\begin{aligned}&\|\sum_{i\in N_h}\{H_i(z)\cdot z^{-N_s^i}[1-\lambda_i\cdot z^{N_s^i}\cdot G_{ip}(z)\cdot Q_f(z)]\}\|<1\\&\forall z=e^{j\omega T_s},\ 0<\omega<\frac{\pi}{T_s}\end{aligned} \tag{4}$$

where T_s is the sample time. Since DFT provides excellent selectivity compared with other algorithms, zero attenuation and zero phase-shift at selected frequency is achieved while gain at other frequencies is attenuated rapidly. Thus, interferences among different harmonics can be neglected to simplify condition (4). As shown in Fig.5, $H_i\cdot z^{-N_s^i}\to 1$ when $\omega\to i\frac{2\pi}{N\cdot T_s}$. Because $G_{ip}(z)$ usually shows low-pass-filter property, the worst case of condition (4) happens in the vicinity of harmonics need to be restrained. In view of the above, condition (4) can be simplified as follows,

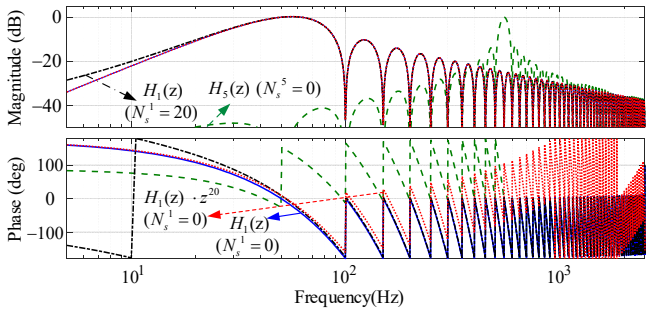

Fig.5: Bode diagram of DFT

$$\begin{aligned} &\| 1-\lambda_i \cdot z^{N_s^i} \cdot G_{ip}(z) \cdot Q_f(z) \| < 1 \\ &\forall z = e^{j\omega T_s},\ i\frac{2\pi}{N \cdot T_s} - \delta < \omega < i\frac{2\pi}{N \cdot T_s} + \delta \end{aligned} \tag{5}$$

where δ is half of the interval length around the desired harmonics, in which the worst case might happen. Suppose that $G_{ip}(z)=\psi_{ip}(\omega)e^{j\theta_{ip}(\omega)} \cdot (1+\Delta z)$, $Q_f(z)=\psi_f(\omega)e^{j\theta_f(\omega)}$, and $1+\Delta z=\sqrt{1+2\|\Delta z\|\cos\theta_\Delta(\omega)+\|\Delta z\|^2}e^{j\theta_\Delta(\omega)}$, then condition (5) leads to the following results,

$$\begin{aligned} &0 < \lambda_i \cdot \psi_{ip}(\omega) \cdot \psi_f(\omega) < \\ &\frac{2\cos[\theta_{ip}(\omega)+\theta_f(\omega)+\frac{2\pi}{N}N_s^i \cdot \frac{\omega}{\omega_0}+\theta_\Delta(\omega)]}{1+\varepsilon} < \\ &\frac{2\cos[\theta_{ip}(\omega)+\theta_f(\omega)+\frac{2\pi}{N}N_s^i \cdot \frac{\omega}{\omega_0}+\theta_\Delta(\omega)]}{\sqrt{1+2\|\Delta z\|\cos\theta_\Delta(\omega)+\|z\|^2}} \end{aligned} \tag{6}$$

where ω_0 is the fundamental angular frequency.

B. Design consideration

It can be easily obtained from inequality (6) that if $\theta_{ip}(\omega)+\theta_f(\omega)+\frac{2\pi}{N}N_s^i \cdot \frac{\omega}{\omega_0}+\theta_\Delta(\omega)=0$, $\lambda_i \cdot \psi_{ip}(\omega) \cdot \psi_f(\omega)$ can vary in the maximum range. Therefore, constraint condition (7)(a) is recommended to strengthen the adaptive ability to variation of $\lambda_i \cdot \psi_{ip}(\omega) \cdot \psi_f(\omega)$ around expected harmonic. On this basis, if $\lambda_i \cdot \psi_{ip}(\omega) \cdot \psi_f(\omega)=1$ and $\Delta z=0$, the denominator of $G_e(z)$ is equal to one and the dynamic response of system at desired harmonic mainly depends on the terms in the numerator of the DFT transform. Since dynamic response time of DFT is at least one fundamental cycle [5], best transient performance is achieved theoretically if both constraint condition (7)(a) and (7)(b) is met. However, constraint condition (7)(a) is hard to achieve in practice due to model error. Thus, enlargement of λ_i may contribute to the convergence speed of system. But constraint condition (b) is still recommended to ensure the stability owing to the limited range of $\lambda_i \cdot \psi_{ip}(\omega) \cdot \psi_f(\omega)$ given in (6). The design effort is to meet the constraint condition (7)(a) and (7)(b) as far as possible.

$$\left.\begin{aligned} N_s^i &= -[\theta_{ip}(\omega)+\theta_f(\omega)] \cdot \frac{N}{2\pi \cdot i} \quad \text{(a)} \\ \lambda_i &= \frac{1}{\psi_{ip}(\omega) \cdot \psi_f(\omega)} \quad \text{(b)} \end{aligned}\right\} \quad \omega = \frac{2\pi}{N \cdot T_s} \cdot i \tag{7}$$

However, it should be pointed out that the leading phase provided by DFT transform $H_i(z)$ is only effective around the desired harmonics, as shown in Fig.5. Hence, corrective function $Q_f(z)$ is needed to provide overall phase compensation within the range of focused harmonics. Furthermore, $Q_f(z)$ is used for correcting control plant to achieve zero attenuation and zero phase-shift at low and medium frequencies as far as possible, while attenuation at medium and high frequencies is needed to suppress switching noise. It makes control system easier to meet the constraint condition (7)(a) and (7)(b).

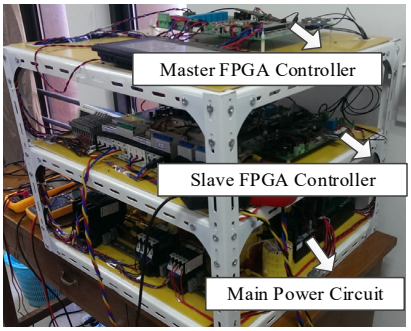

Fig. 6: Experimental setup

IV. Experimental Results

In order to verify the effectiveness of the proposed enhanced controller, experimental setup shown in Fig.6 is built in the laboratory to verify the theoretical analysis. The specific APF parameters have been listed in Table 1. Since typical three-phase diode rectified bridge is used here as the nonlinear load, the harmonic spectrum contains only harmonics of orders $k=6n\pm1$ [7]. So only harmonics of orders $k=6n\pm1$ are selected in the experiments.

Power analyzer (WT1800 from YOKOGAWA Corporation) is used to measure the total harmonic distortion (THD) and harmonic spectrum of grid current.

The traditional repetitive-based DFT controller and the proposed controller are both performed in the master control board while the current and voltage loop are performed in the slave control board. For DFT, N is set to be 768.The communication delay between master and slave control board

Table. 1: APF parameters

DC Link Voltage	430V
Switching frequency f_s	10KHz
Line voltage (rms)	220V
Fundamental frequency	50Hz
Filter Inductor L_f	3.22 mH
R_f	0.1Ω
Selected harmonic frequencies N_h	3^{rd},5^{th},7^{th},11^{th}, 13^{th},15^{th},17^{th},19^{th}, 23^{th},25^{th},29^{th},31^{th}, 35^{th},37^{th},41^{th},43^{th}

is 20us. $Q_f(z)$ with unit gain coefficient has two poles at 10KHz and one zero at 2KHz, which is used to correct the plant for better characteristics. The sampling time T_s of current loop is 100us and digital control delay time is 150us. Proportional-integral algorithm is adopted for the current loop with bandwidth of 500Hz and 45°phase margin. Optimized design consideration is adopted in the proposed controller, while two steps of leading angle is provided in the traditional controller, as mentioned in literature [3].

Fig.7(a) illustrates that the proposed controller still has excellent selectivity. The magnitudes of 5th harmonic before and after compensation are 1.923A and 0.036A respectively.

Fig.7(b) shows good compensation performance achieved by the proposed controller. THD of grid current before and after compensation are 26.114% and 2.663% respectively. Besides, the residual current of each harmonic frequency is less than 0.04A, as illustrated in Table.2. The amount of residual harmonic currents relate with the accuracy of the digital implementation of the DFT.

Comparisons between Fig.8(a) and Fig.8(b) illustrate that the proposed controller achieve wider stability margins than the traditional controller. The grid current in Fig.8(a) is already unstable.

As shown in Fig.8(b), the response time of proposed controller is around 1.8 line periods, which can be furtherly improved if model uncertainty is accurately estimated in practice.

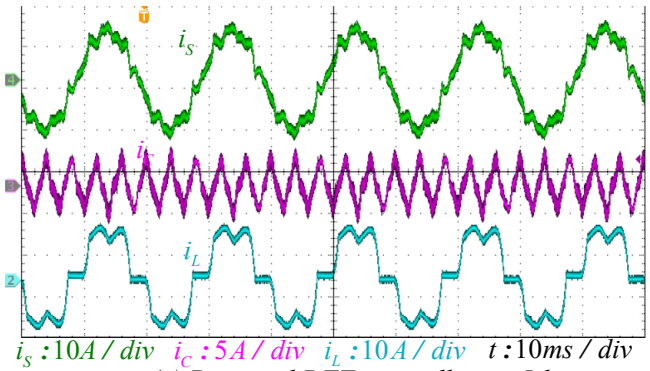

i_S : 10A / div i_C : 5A / div i_L : 10A / div t : 10ms / div

(a) Proposed DFT controller, $i = 5th$

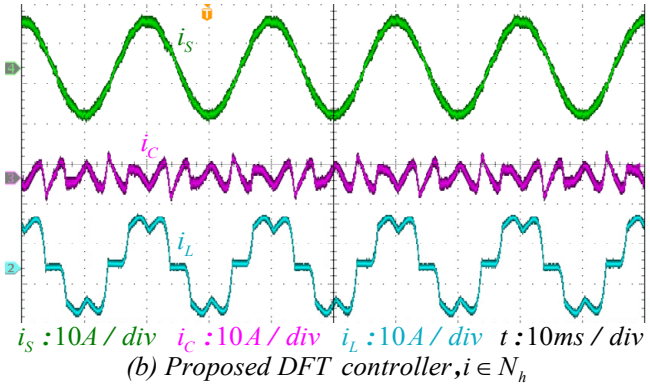

i_S : 10A / div i_C : 10A / div i_L : 10A / div t : 10ms / div

(b) Proposed DFT controller, $i \in N_h$

Fig.7 Experimental waveforms of steady state

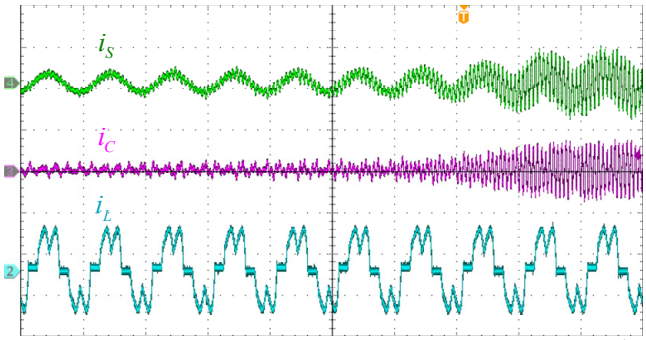

i_S : 20A / div i_C : 20A / div i_L : 5A / div t : 20ms / div

(a) Traditional DFT controller, $i \in N_h$

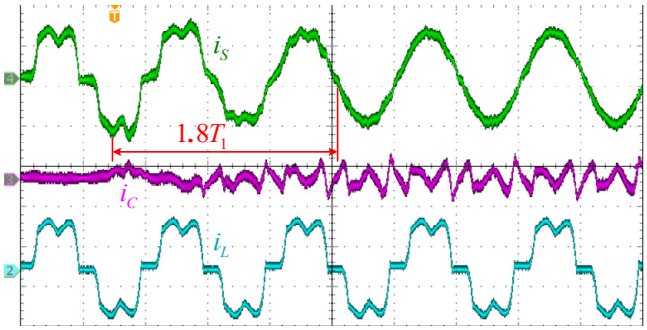

i_S : 10A / div i_C : 10A / div i_L : 10A / div t : 10ms / div

(b) Proposed DFT controller, $i \in N_h$

Fig.8 Experimental waveforms of transient behavior

Table. 2: Harmonic Spectrum of grid current

Harmonic order	Before compensation(rms)/A	After compensation(rms)/A
1st	8.018	8.245
3rd	0.112	0.005
5th	1.900	0.036
7th	0.630	0.031
11th	0.464	0.026
13th	0.261	0.025
17th	0.187	0.011
19th	0.109	0.011
23th	0.104	0.013
25th	0.067	0.016
29th	0.069	0.029
31th	0.051	0.026
35th	0.039	0.026
37th	0.029	0.010
41th	0.034	0.039
43th	0.018	0.021

V. CONCLUSIONS

A novel enhanced DFT-based controller is proposed in this paper. The proposed controller provides feedback path and gain coefficient for each harmonic. Hence, it is able to compensate the phase lag and tune the gain according to the frequency characteristics of the plant at different harmonics respectively compared with previous approaches. Based on the stability analysis, optimized design consideration is given to make full use of the advantages of the proposed controller. The effectiveness and advantages of the proposed controller have been verified by the experimental results. It not only has the advantages of better compensation performance and excellent selectivity but also achieves good transient performance, which is very suitable for the application of selective harmonic compensation.

REFERENCES

[1] Yi, Hao, et al, "A Source-Current-Detected Shunt Active Power Filter Control Scheme Based on Vector Resonant Controller," *IEEE Transactions on Industry Applications* 50.3(2014):1953-1965.

[2] Mattavelli, P, "A closed-loop selective harmonic compensation for active filters," *IEEE Transactions on Industry Applications* 37.1(2000):81-89.

[3] Mattavelli, P., and F. P. Marafao, "Repetitive-based control for selective harmonic compensation in active power filters," *IEEE Transactions on Industrial Electronics* 51.5(2004):1018-1024.

[4] Lascu, Cristian, et al, "Frequency Response Analysis of Current Controllers for Selective Harmonic Compensation in Active Power Filters," *IEEE Transactions on Industrial Electronics* 56.2(2009):337-347.

[5] Liserre, M., R. Teodorescu, and F. Blaabjerg, "Multiple harmonics control for three-phase grid converter systems with the use of PI-RES current controller in a rotating frame," *IEEE Transactions on Power Electronics* 21.3(2006):836-841.

[6] Mattavelli, P, " Synchronous-frame harmonic control for high-performance AC power supplies," *IEEE Transactions on Industry Applications* 37.3(2001):864-872.

[7] Lascu, Cristian, et al, "High Performance Current Controller for Selective Harmonic Compensation in Active Power Filters," *IEEE Transactions on Power Electronics* 22.5(2007):1826-1835.

[8] Huawu Liu, Haibing Hu, Hao Chen, et al, "Fast and Flexible Selective Harmonic Extraction Methods Based on the Generalized Discrete Fourier Transform," *IEEE Transactions on Power Electronics* PP.99(2017):1-1.

[9] Limongi, Leonardo Rodrigues, et al, "Digital current-control schemes," *IEEE Industrial Electronics Magazine* 3.1(2009):20-31.

[10] Jacobsen, E, and R. Lyons, "The sliding DFT," *Signal Processing Magazine IEEE* 20.2(2003):74-80.

[11] Jacobsen, Eric, and R. Lyons, "An update to the sliding DFT," *IEEE Signal Processing Magazine* 21.1(2004):110-111.

[12] Mcgrath, B. P., D. G. Holmes, and J. J. H. Galloway, "Power converter line synchronization using a discrete Fourier transform (DFT) based on a variable sample rate, " *IEEE Transactions on Power Electronics* 20.4(2005):877-884.

[13] Duda, Krzysztof, "Accurate, Guaranteed Stable, Sliding Discrete Fourier Transform [DSP Tips & Tricks]," *IEEE Signal Processing Magazine* 27.6(2010):124-127.

[14] Neves, Francisco A. S., et al, "A Space-Vector Discrete Fourier Transform for Unbalanced and Distorted Three-Phase Signals," *IEEE Transactions on Industrial Electronics* 57.8(2010):2858-2867.

[15] Geiselhart, R, M. Lazar, and F. R. Wirth, "A Relaxed Small-Gain Theorem for Interconnected Discrete-Time Systems," *Automatic Control IEEE Transactions on* 60.3(2015):812-817.